PHYSICAL REVIEW B VOLUME 24, NUMBER 12 15 DECEMBER 1981

Single-ion-pair fluorescence ratios in ruby and Anderson localization

S. Chu, H. M. Gibbs, and A. Passner
Bell Laboratories, Murray Hill, New Jersey 07974
(Received 8 October 1980; revised manuscript received 8 June 1981)

The experiment of Koo, Walker, and Geschwind (KWG) presenting evidence for a mobility edge separating localized and extended states has been repeated and extended. Although some of the features reported by KWG were seen, there are notable qualitative and quantitative differences in our work. We conclude that there is no compelling evidence for an Anderson transition in ruby.

I. INTRODUCTION

Since the development of the laser, a great deal of attention has been paid to understanding static and dynamic spectral details of ruby (Al_2O_3: Cr^{3+}). Energy transfer studies have become particularly significant in light of an experiment by Koo, Walker, and Geschwind[1] (KWG) which reported the observation of an Anderson mobililty edge.[2] In spite of a great deal of work on conduction in amorphous systems, inversion layers, impurity-band semiconductors, and exciton mobility in organic crystals,[3–5] the subject is haunted by a lack of unambiguous evidence for this edge.

Rapid single-ion–single-ion transfer in ruby was postulated by Imbusch[6] who compared the R_1 fluorescence lifetimes at 6934 Å to pair (trap) fluorescence decays at 7009 Å (N_2 line) and 7041 Å (N_1 line) corresponding to fourth- and third-nearest-neighbor pairs, respectively. He concluded that the identical lifetimes of the 6934, 7009, and 7041 Å fluorescence and the large absolute values of the 7009 Å fluorescence could be explained best by postulating a rapid single-ion–single-ion transfer, which he estimated to take on the order $1-10$ μsec for 1 wt. % ruby, that could feed the trap states. The necessity for fast single-ion transfer was also stressed by Selzer *et al.*[7] based on similar studies. Birgeneau[8] suggested that the energy-transfer mechanism is dominated by a short-range (exponential) anisotropic exchange interaction, and suggested a characteristic transfer rate to be $\cong 10^7$ sec^{-1} in 1 wt. % ruby. Recently, Monteil and Duval[9] obtained evidence favoring single-ion–single-ion transfer with an exponential range behavior.

Based on the earlier transfer studies, Lyo[10] analyzed transfer in ruby using Anderson's ideas,[11,12] and predicted a critical concentration of $\sim 0.3-0.4$ wt. % Cr which would mark the separation between localized and extended states in ruby. In an elegant experiment, Koo, Walker, and Geschwind[1] used the ratio of the trap fluorescence at 7009 Å to single-ion fluorescence at 6934 Å as a monitor of the mobility of the exciton states. They argued that localized states could not transfer their energy to the trap states as easily as the extended states and that if the concentration of the ruby were correctly chosen, the inhomogeneously broadened R_1 line in a particular sample would have regions of localized and extended states. They observed N_2/R_1 emission in several concentrations ranging from 0.05% to 1.4%. In the ruby concentrations of 0.09, 0.14, and 0.23 wt. % they report an essentially flat N_2/R_1 ratio followed by a fairly sharp drop to a lower N_2/R_1 ratio as the wavelength of a narrow-band ruby laser was tuned from line center to the longer wavelength side of the inhomogeneous R_1 line. The region in the inhomogeneous line where the drop occurred moved away from line-center as the concentration was increased, and for 0.05 and 1.4 wt. % concentrations, no change in the N_2/R_1 ratio was observed. This suggested that at these concentrations the states are only localized or only extended, respectively.

The status of energy transfer in ruby is by no means settled, and many seemingly conflicting results have been reported. Heat-pulse measurements of Heber and Murmann[13] at 5.3 K have been interpreted to show that only phonon-assisted energy transfer exists in ruby, instead of the resonant energy transfer postulated in the KWG experiment. Single-ion transfer times were measured to be on the order of 250 μsec for 1.35 wt. % doped ruby. Phonon-assisted transfer within the inhomogeneous R_1 line has been seen in careful studies by Selzer *et al.*[7] in a temperature range $5-80$ K and in a concentration range

0.03 – 1.0 wt. % ruby. Alternatively, Szabo[14,15] sees no evidence of phonon-assisted transfer at $\cong$4.2 K in 0.05 and 0.1 wt. % concentrations. Gerlovin[16] has studied R_1, N_1, and N_2 fluorescence and has come to the conclusion that the behavior of these fluorescent lines is not compatible with rapid energy migration in ruby. Transient grating work by Laio *et al.*,[17] Hamilton *et al.*,[18] and Eichler *et al.*,[19] show no spatial diffusion of the Cr^{3+} excitation down to a scale of $\gtrsim$300 Å for a wide range of concentrations. Finally, although Selzer *et al.*[7] believe that fast resonant transfer between single ions does occur, they see no dramatic change in the single-ion – single-ion energy-transfer properties as a function of laser excitation frequency.

In view of the importance and seemingly conflicting results associated with energy transfer in ruby, we decided to repeat and extend the KWG experiment. One obvious extension of their experiment would be the ability to selectively excite Cr^{3+} ions both on the blue and red wavelength sides of the inhomogeneously broadened line. If a similar break-like feature in the N_2/R_1 ratio were observed on both sides of the line, the case for an Anderson transition in ruby would be strengthened. The extension would also directly address a criticism of Selzer *et al.*,[7] who suggest that the asymmetric inhomogeneous distribution in ruby at the concentrations of interest may be the result of weak clustering of Cr^{3+} ions that create a class of "abnormal" ions peculiar to the red wavelength sides of the R_1 line.

A. Experimental Details

The schematic of experimental apparatus is shown in Fig. 1. A Kr-ion laser was used to pump an amplitude stabilized cw dye laser. A dilute concentration of $\cong$120 mg of Oxazine 725 in 750 ml of ethylene glycol resulted in ample tunable laser power in the 6934 Å region. Typically, the dye laser was run in two longitudinal modes separated by $\cong$1.6 GHz, with some mode jitter so that the time averaged linewidth is $\cong$3 GHz, but single longitudinal mode operation was possible with the use of a 1-cm-thick temperature-tuned etalon. The laser was constantly monitored with a Fabry Perot etalon in conjunction with a He-Ne reference laser.

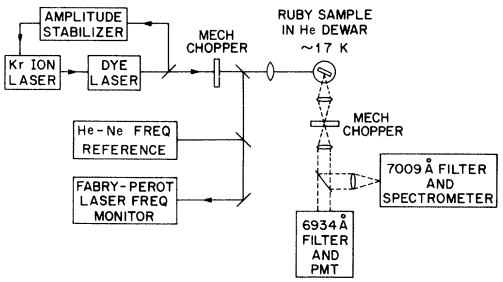

FIG. 1. Schematic representation of the apparatus is shown. Spectrometer resolution was typically set at $\Delta\lambda \simeq 1.5$ Å, but higher resolution data showed no change in the N_2/R_1 ratios.

The ruby samples were thin platelets or single layers of ruby powder immersed in liquid helium. The sample temperature was nominally 1.7 K as monitored by the helium pressure in the Dewar, but by observing the ratio of the R_1 and R_2 emission lines separated by 29 cm^{-1} when we excited with a cw laser tuned to the R_1 frequency, the temperature in the sample due to laser heating was determined to be $\lesssim$3.7 K. Typically, laser intensities of $\simeq$1 mW average power were delivered to the sample in a focal spot size of $\simeq$1 mm^2. At these low light levels, only a small fraction of the Cr^{3+} ions were excited, and the saturation of the N_2 traps due to energy transfer single ions was avoided. We eliminated the possibility of trap saturation as well as the possibility that our detectors or counting electronics were nonlinear by observing no change in the N_2/R_1 ratio near the center when the laser intensity was reduced by roughly a factor of 100. In another test of our system, we tuned the spectrometer to 7016 Å so that we were observing the phonon side band of the R_1 decay. As the laser was tuned in the vicinity of 6934 Å, the 7016 Å/6934 Å fluorescence ratio did not change as a function of laser wavelength.

A mechanical chopper was used to square-wave modulate the incident laser light in a square-wave modulation such that the light radiated the sample for 20 ms and was blocked for 20 ms. During the time the laser beam irradiated the sample, we found that a second mechanical chopper was necessary to prevent the saturation of the phototubes (RCA 8852 tubes cooled to -40 °C) from scattered laser light. Saturation of our detectors and/or counting electronics when the laser beam was hitting the sample resulted in a several millisecond recovery time that distorted the true N_2/R_1 ratio. This distortion was particularly bad when we used ac-coupled amplifiers between the phototubes and scalars, and sometimes caused spurious changes in the N_2/R_1 ratio. A beam splitter directed $\simeq$30% of the fluorescent light to a phototube and 6934 Å interference filter [10 Å full

width at half maximum (FWHM)] while the remainder of the light was focused into a 1 m spectrometer. A 7009 Å interference filter was used in series with the spectrometer.

The experimental arrangement shown in Fig. 1 was not used to measure the absolute value of the N/R ratios. Instead, the beam splitters, apertures, etc., were used to adjust the counting rates of the $N_{1,2}$ detector and R_1 detector so that they were comparable. Since we were searching for sudden changes in the N/R ratio, we felt that only the relative fluorescence intensities were important. For example, if the absolute value N/R ratio were changed by a factor of 3 but a sharp break could be seen, the break would still be consistent with the KWG interpretation. Later, separate absolute measurements of the N/R ratio were made by directing all the light into the spectrometer/ photomultiplier detector, and tuning the spectrometer alternately between the N_2 line and the R_1 line. The specified phototube spectral response decreases by less than 10% between 6934 and 7009 Å and the grating was blazed for a maximum efficiency at 7000 Å, so no correction to the fluorescence ratio was made. The N_2/R_1 ratios of our 0.25, 0.69, and 1.2 wt. % samples were measured to be 10^{-2}, 2×10^{-1},and 8×10^{-1}, respectively, with perhaps a 20% relative error. These ratios are consistent with the data of Imbusch[6] and KWG.[1]

Fluorescence data presented in this paper were taken by counting single photons collected between 5 and 25 msec after the laser beam was blocked. Longer delays between pulse turn-off and counter turn-on did not affect the general character of the N_2/R_1 rates, but shorter delays changed the ratios significantly when the laser frequency coincided with a trap absorption. The changes can be ascribed to the direct excitation of identified excited states of the N_2 trap spectra[20] and their rapid $\simeq$0.8 ms decay, or to a fast feeding of single ions close to traps. The 5 ms delay after the end of laser excitation allowed us to look at only the trap emission that is the result of a transfer of energy from a single ion to a trap. A similar timing sequence was also used in the KWG experiment.

Radiative trapping could play a significant role in the determination of the N_2/R_1 ratio. For example, suppose a Cr^{3+} ion is excited, but for some reason it has little chance to transfer nonradiatively to a trap. Under radiative trapping conditions, the ion could transfer its excitation by emission and absorption of a real photon to another microscopically random site which might be able to transfer to a trap. As the laser is tuned from line center, the probability that a 6934 Å fluorescence photon will be reabsorbed will decrease, and consequently the N_2/R_1 ratio will decrease. We avoided reabsorption of R_1 light by using particles of ruby as our samples. Ruby powder of a given size was made by crushing a sample of known concentration in an agate mortar and filtering the powder in a series of fine mesh filters with mesh sizes between 5 and 50 μm. The particle sizes were measured using a calibrated optical microscope after a *submonolayer coating* of ruby powder was deposited on a microscope cover slide.

The concentration of Cr ions (by weight of Cr) in our samples was determined by measuring the ratio Cr—Kα x-ray fluorescence from an unknown sample and a standard sample of known concentration. By measuring the concentration of two pieces from the same ruby boule, the relative accuracy of this technique is estimated to be roughly 10 wt. %.

II. EXPERIMENTAL RESULTS

Figures 2 and 3 show the N_2/R_1 ratios and R_1 fluorescence as a function of laser detuning from line center. As in the KWG experiment, only the relative ratios are shown. Unless noted otherwise, the zero value of the N/R ratio coincides with the intersection with the x axis. Least-squares fits of the decay curves give $\bar{E}$ lifetimes of 3.7 ms for the 3 and 20 μm size particles and show a 10% increase of the lifetime in the 40 μm sample. Our value of 3.7 ± 0.08 ms for the intrinsic lifetime of ruby at moderate concentrations agrees with the values given by Selzer and Yen[21] and by Liao *et al.*[17] Thus we are confident that our 3 and 20 μm size particles can not be significantly radiatively trapped. The immediately obvious result of Figs. 2 and 3 is that the shape of the curve of N_2/R_1 ratio versus detuning remains essentially the same for the different size samples despite the changes in the R_1-line inhomogeneous width. Since all the powder samples were made from the same section of a single ruby boule, the increase in the inhomogeneous linewidth is probably due to a macroscopic strain-induced broadening that results from the crushing procedure. (Smaller powders would recieve more strain.) One could argue that each separate particle in the sample could have a strain-shifted and broadened line shape as a result of the sample preparation, and any sharp features

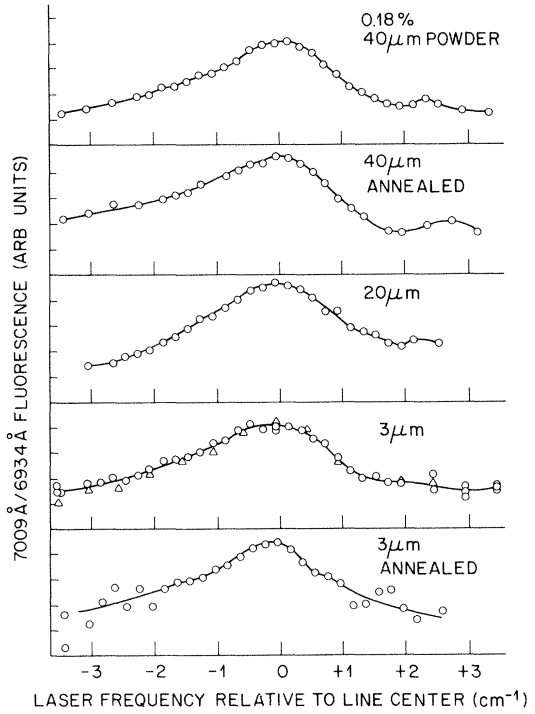

FIG. 2. N_2/R_1 fluorescence ratios as a function of laser detuning from line center of the R_1 inhomogeneous absorption profile for various particle sizes. (All $N_{1,2}/R_1$ and R_1 curves are plotted on a relative linear scale with the zero value intersecting the x axis unless otherwise noted. Also, negative frequency units represent frequencies to the red of line center.)

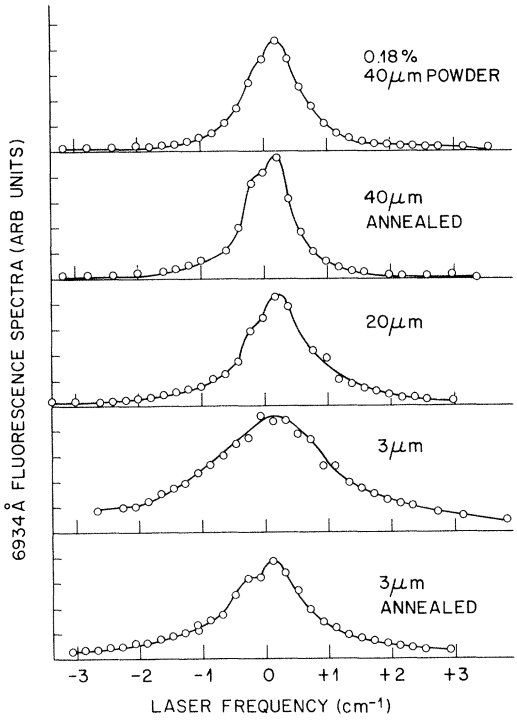

FIG. 3. R_1 inhomogeneous line shapes corresponding to the N_2/R_1 ratios in Fig. 2. The 0.38 cm^{-1} ground-state splitting of ruby is partially resolved in all but the 3 μm unannealed powder.

in the N_2/R_1 ratio would have been washed out. Consequently, some of the samples were annealed, typically for 2 h at 1300° C, to remove the additional macroscopic strain, and the decrease in linewidth is shown in the R_1 linewidths in Fig. 3. The lifetimes in these samples were also 3.7 ms. Again no qualitative change in the N_2/R_1 ratios in Fig. 2 was observed.

Other sample concentrations were measured with the same procedure and are shown in Fig. 4. The general features in the N_2/R_1 ratio seen in Fig. 2 are repeated in Fig. 4, despite the order-of-magnitude change in concentration. Some of the powder data were taken in samples that showed a slight amount of radiative trapping, as measured in the R_1 decay lifetimes, but we believe that the work on the 0.18 wt. % samples indicates that a 10 wt. % increase in the lifetime does not change the essential character of the N_2/R_1 curves.

Small ruby platelet samples were also studied and some representative results are shown in Fig. 5. One reason for considering platelets is that annealing does not completely remove the macroscopic strain induced in the preparation of the powder samples, and possibly the sharp break-like features would be obscured by a smooth distribution of sharp features at slightly different wavelengths. The inhomogeneous linewidths of the platelet samples were in fact narrower by approximately a factor of 2 from the powder data of comparable concentration. However, sudden changes in the N_2/R_1 ratio failed to appear. Also, the resonant-like peak at $\cong 2.5$ cm^{-1} to the blue of line center sharpened considerably as compared to the powder data.

Two important points should be mentioned in reference to the platelet data. First, we had difficulty in obtaining samples free from radiative trapping. Our attempts to reduce the thickness of the crystal below $\cong 50$ μm using conventional polishing techniques often shattered the crystal. A series of experimental runs was made on a 0.17 wt. % sample starting at a thickness of 40 μm. After the first run the sample was Ar-ion milled to 20 μm and finally to $\simeq 10-15$ μm. The R_1 lifetime decreased from 6.2 to 4.6 ms compared to the 3.7 ms

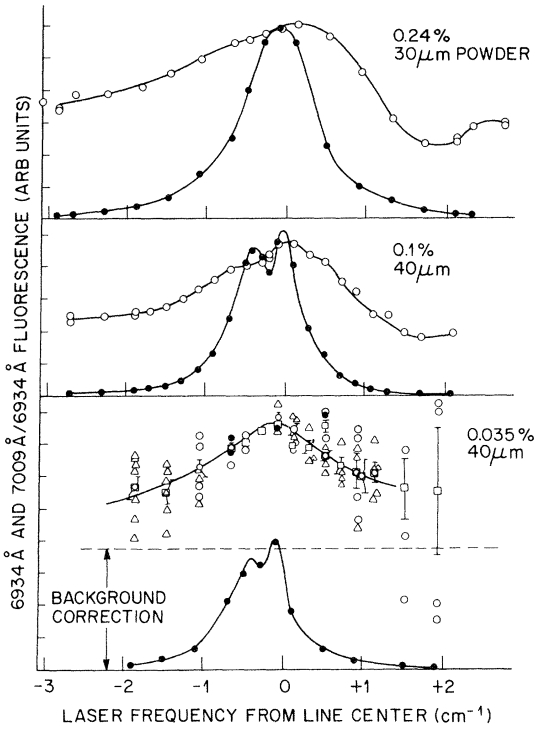

FIG. 4. R-line inhomogeneous line shapes and N_2/R_1 ratios for powder samples of several concentrations are shown. The 7009 Å fluorescence varies as c^3 where c is the concentration of Cr ions in ruby, thus making N_2/R_1 ratio measurements in the 0.035 wt. % sample difficult. The background correction is due mainly to phototube dark counts and phonon-assisted R_1-line decays.

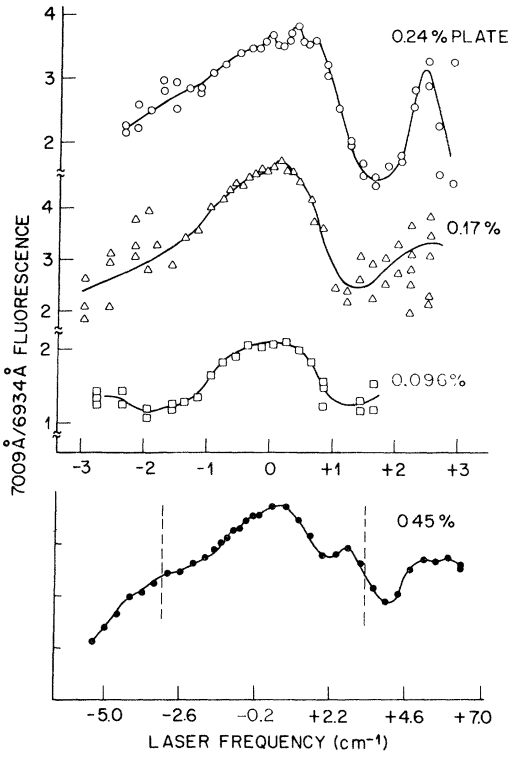

FIG. 5. N_2/R_1 fluorescence ratios for various platelet concentrations are shown. The zero for the vertical axis has been suppressed. Note that the general features of the N_2/R_1 curve are repeated in the 0.45 wt. % sample in the region -3 to $+3$ cm^{-1} from line center.

untrapped lifetime. As with the powder data at 0.18 wt. %, there was no significant change in the N_2/R_1 ratio. Note that the 20 μm powder sample at 0.17 wt. % did not show radiative trapping because of the substantially broader inhomogeneous linewidth. Also, part of the radiative trapping is *reflective* trapping that occurs when photons in the sample are reflected at the ruby-helium interface. We expected reflective trapping to be larger in our plate samples. Unfortunately, the ion-milling procedure proved to be awkward and expensive, so most of the platelet data were taken on radiatively trapped samples. The work on the 0.17 wt. % sample shows that radiative trapping, even enough to produce a 6.2 ms lifetime, does not significantly alter the N_2R_1 ratio. The second point worth mentioning is that platelet data were not as reproducible as the powder data. Figures 6 and 7 show examples of strong deviations from the average of all the data, and Fig. 6 is especially intriguing since it shows a sharp change in the N_2/R_1 ratio reminiscent of the KWG data. However, repeated runs on the same sample did not duplicate this behavior, and the curve shown in Fig. 5 is representative of the rest of the runs. Note that the characteristic frequency width of any N_2/R_1 change measured when the laser is operating with an effective bandwidth of 3 GHz is much greater than the resolution of our experiment, since the R_1 absorption line always shows sharper features than the N_2/R_1 ratio.

We also took a limited number of single frequency (jitter $\simeq$40 MHz) scans on low concentration platelets of 0.035 and 0.99 wt. %. One such scan is shown in Fig. 8. Also included is a scan taken of the same sample, but with the laser operating in the usual multimode fashion. The R_1 fluorescence spectrum actually resolves the Cr^{52}/Cr^{53} isotope shift in the R_1 line. Although there is no sharp structure in the limited tuning range, there are two "resonances" in the N_2/R_1 ratio that are associated with the R_1 peaks, but red

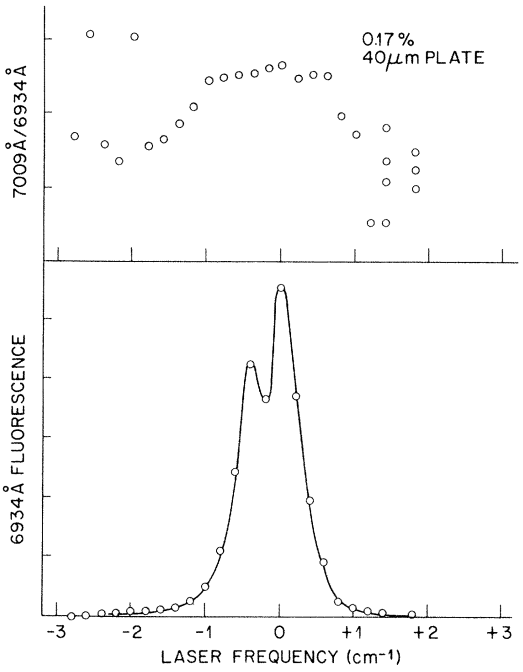

FIG. 6. N_2/R_1 ratio and R_1 line shape for the 0.17 wt. % sample.

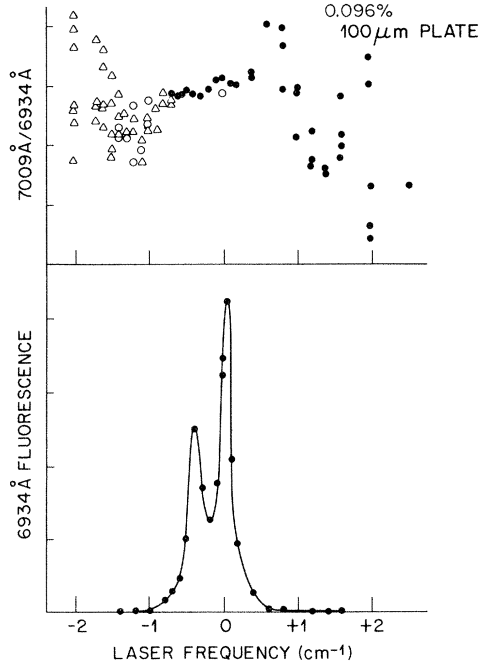

FIG. 7. N_2/R_1 ratio and R_1 line shape for the 0.096 wt. % sample.

shifted by $\simeq 0.1$ cm^{-1}. This result is hard to explain in the framework of the KWG interpretation. Alternately, we speculate that the frequency shift is a result of the correlation between the excitation frequency of a Cr^{+3} ion and its ability to transfer its energy to a trap. We shall argue later that the trap fluorescence is not enhanced by the rapid exchange of energy among single ions, but probably is dominated at these concentrations by direct transfer of nearby single ions to traps. If one assumes this model, then a plausible explanation can be given for the N_2/R_1 shape shown in Fig. 8. The probability of detecting an N_2 fluorescent photon from a trap not directly excited by the laser is simply given by the product of the inhomogeneous R_1 line shape and the probability $P(\omega)$ of transferring energy from R to N. If there is a correlation between the position of any given Cr^{3+} ion in the inhomogeneous line and its distance to a trap [evidence for this correlation can be seen in Fig. 10(b)], $P(\omega)$ will certainly be frequency dependent. If one averages over all single ion-to-trap distances and assumes a $1/r^n$, $n \geq 6$ model for the single ion-to-trap transfer probability, it is possible to obtain a rough fit to the N_2/R_1 ratio curve in Fig. 8. The average is an integral over all distances, r_0 to ∞, where r_0 is some minimum distance cutoff parameter, and time t_1 to t_2 define the time interval where the N_1 and R_1 counts were recorded. Such

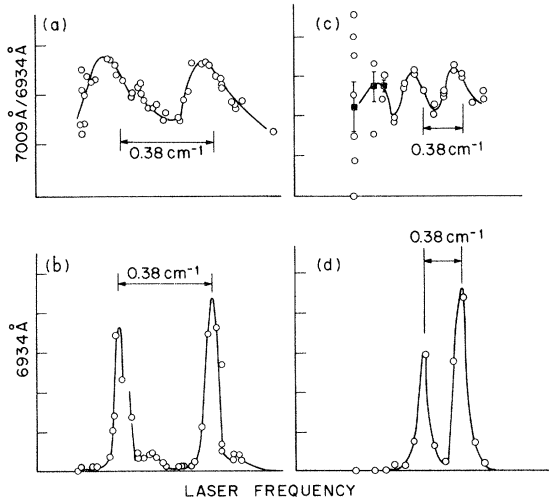

FIG. 8. N_2/R_1 ratio and R_1 line shape for the 0.035 wt. % platelet: (a), (b) under single-mode scan ($\sim$40 MHz) and (c), (d) under the usual laser operating conditions ($\sim$3 GHz). The frequency glich in curves (a) and (b) and the result of a sudden shift in the monitoring Fabry Perot. The error bars in (c) are statistical errors in the mean.

a fit requires that the closer a "single" ion is to a trap, the more likely on average it is red shifted with respect to the center of the inhomogeneous line. Furthermore, the average frequency shift favors a long-range dependence ($n \leq 3$) to fit the N/R ratio line shape. A short-range exchange red shift gives a skewed line shape for the N/R ratio that is weighted heavily towards small frequency shifts.

A summary of the N_2/R_1 data taken with the same timing conditions as the KWG experiment is given in Table I. We define a "break" in the 7009 Å/ 6934 Å ratio and the frequency where it occurs, as indicated in Fig. 9. Although our break seems somewhat artificial, it allows us to compare our data quantitatively with the KWG data, which have also been included in Table I. The errors listed are statistical errors in the mean, averaged for all runs of a particular powder or platelet concentration, regardless of particle size.

We also took N_2/R_1 data for different conditions. In Fig. 10 we show representative data taken on a 0.18 wt. %, 20 μm diameter powder sample. Curve (a) is data taken under the usual timing conditions where the fluorescence ratio is recorded in the time interval 5—14 ms after laser excitation. Curve (b) includes only the fluorescence in the first 0.5 ms after the end of the laser pulse, and curve (c) is the counts in time interval 0—14 ms. Curve (b) has been divided by ten in order to plot curves (a) and (b) on the same scale. Curve (b) exhibits a broad resonance roughly 2 cm^{-1} to the red of the inhomogeneous line center and coincides with a known excited state of the N_2 trap.[20] Using the notation of Kisliuk *et al.*,[20] we are exciting the 4H3 transition. With the laser tuned to the peak of this resonance, the 7009 Å decay shows a submillisecond immediately after the end of the laser excitation that agrees with the 7009 Å trap lifetime. This is a clear signature of direct laser excitation of the trap states. However, when the laser is tuned to line center, the initial decay has a lifetime slope of roughly 2.4 ms. We identify the initial decay as the feeding of the N_2 traps states by single ions in their near vicinity. Curve (b) indicates that the near-neighbor single-ion feeding to the N_2 trap is slightly higher for those ions with R_1 frequencies towards the red side of the inhomogeneous line. This result, which is also consistent with Fig. 8, is not surprising since there appears to be a general shift toward red frequencies when Cr ions interact with each other in ruby. Ions close to traps will have, on average, frequencies that are slightly red shifted. We feel this correlation explains the single-mode data shown in Fig. 8.

Clearly, the character of the N_2/R_1 fluorescence ratio is changed if we also include the first 5 ms of the N_2 and R_1 decays. More importantly, the feeding of traps by single ions in the first few milliseconds after excitation gives a decay curve that is *not single exponential.* Historically, the basis for postulating rapid single-ion—single-ion transfer has come from the single exponential decay of the 7009 Å fluorescence at a rate equal to the 6934 Å single-ion fluorescence.[6,7] However, our studies in nonradiatively trapped powder samples in a variety of concentrations have shown that the N_2 fluorescence decays at a faster rate than the R_1 fluorescence, especially at early times, and only after a few R_1 decay times do the N_2 and R_1 decay rates approach each other. Our results have prompted us to reexamine the need for rapid single-ion—single-ion transfer since the 7009 Å flourescence decay rate is not a single exponential decay. The data and these results will be presented in a later paper.[22]

III. DISCUSSION OF DATA

The N_2/R_1 data can be characterized by a universal curve, but with some apparent systematic differences. The $+2.5$ cm^{-1} peak is smaller or lost in the noise at low concentrations, especially in the powder data, but becomes sharper and more pronounced in crystal samples of high concentration and narrower inhomogeneous linewidths. In the platelet data there is additional structure near line center that is more pronounced in the single-mode laser runs at 0.035 and 0.096 wt. %. (Note that our low-concentration platelets show very narrow inhomogeneous broadening: 0.18 cm^{-1} FWHM for the 0.096 wt. % sample and 0.07 cm^{-1} FWHM for the 0.035 wt. % sample.) This structure may reflect the effects of radiative trapping, but is more likely due to the frequency-position correlation previously discussed. Also, even though radiative trapping should affect the N_2/R_1 ratio at some level, its effect would be a monotonically decreasing function symmetric about line center. Thus, the appearance of three or more bumps in the N_2/R_1 data, and certainly the resonance at $+2.5$ cm^{-1} can not be explained by trapping.

Obviously, we failed to observe the sharp breaks presented in the KWG experiment. In addition, the

TABLE I. Summary of N_2/R_1 fluorescence versus laser frequency.

Concentration C (% dry wt)	Particle size or plate thickness (μm)	$\Gamma_{inhomog}$(HWHM) linewidth (cm^{-1})	No. of runs	Half point of "break" (cm^{-1})		Break/Γ		C/Γ(%/cm^{-1})
				Blue side	Red side	Blue side	Red side	
Powder data								
0.035	40	0.3	3	1.03±0.15	0.87±0.16	3.5±0.9	3.0±0.75	0.12
0.1	40	0.4	2	1.04±0.20	0.9 ±0.14	2.6±0.6	2.7±0.02	0.25
0.18	22040	0.25−1.0	10	1.1 ±0.08	1.1 ±0.08	2.4±0.19	2.6±0.34	0.18−0.72
0.24	30	0.45	5	0.98±0.09	1.1 ±0.08	2.3±0.17	2.5±0.29	0.053
Platelet data								
0.096	75100	0.22	6	0.87±0.08	0.69±0.04	6.0±2.2	5.0±0.7	0.44
0.17	152040750	0.2−0.4	16	0.88±0.04	0.91±0.03	3.7±0.3	3.6±0.2	0.43 to 0.85
0.20	100	0.3	3	1.1 ±0.1	0.95±0.05	3.75	3.22	0.67
0.24	1000	0.2	1	0.75	0.7	3.75	3.5	1.2
0.45	450	0.6	1	0.8	1.1	1.43	1.69	0.75
KWG data								
0.05					No break			
0.09		0.4			0.3		0.75	0.23
0.14		0.7			1.0		1.4	0.2
0.23		1.3			1.5		1.15	0.18
0.5					No break			
1.4					No break			

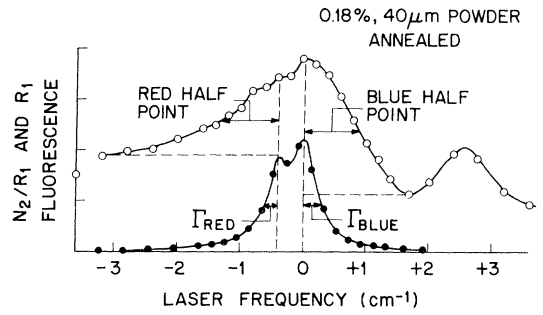

FIG. 9. Definition of the terms used in Table I. Note that the frequency region to the red of line center bears some resemblance to the KWG data.

contrast between the peak of the N_2/R_1 ratio and the lower values is a factor of 2 or greater than their results. (Recall that $\simeq$40% drop is seen in their 0.09 wt. % sample, but only a $\simeq$15% drop is seen in the 0.23 wt. % sample.) The position of our breaks as defined in Fig. 9 does not vary with concentration as in the KWG data, but remains fixed at roughly 1 cm^{-1} to either side of the two R_1 lines. Our data are compatible with a concentration-independent N_2/R_1 curve. We see a drop in the N_2/R_1 ratio in the 0.035 wt. % powder sample that is consistent with the higher concentration curves, even though KWG report a flat N_2/R_1 ratio in their 0.05 wt. % sample. Similarly, our 0.45 wt. % plate sample exhibits the same "universal" structure while the KWG experiment reports no break. Thus, we conclude that our N_2/R_1 ratio data do not provide any evidence for a sharp mobility edge.

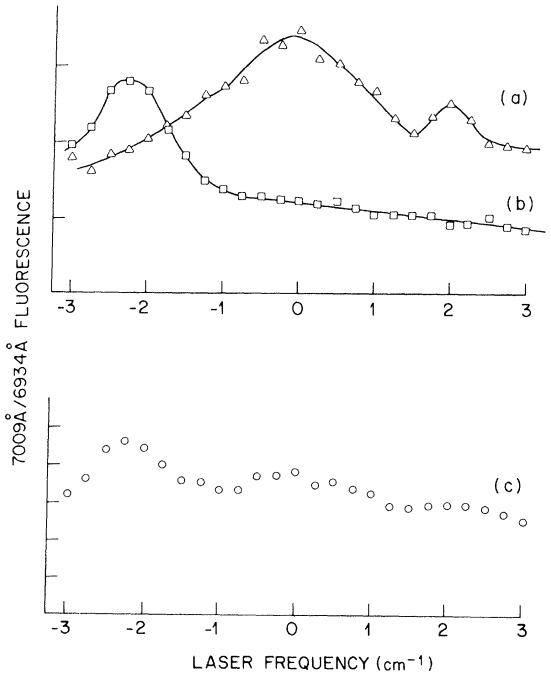

FIG. 10. N_2/R_1 fluorescence ratio as a function of laser frequency for different counting intervals after laser excitation. Curve (a) is a N_2/R_1 ratio for 0.18 wt. % ruby powder taken under the usual timing conditions. Curves (b) and (c) show N_2/R_1 for time intervals 0–0.5 msec and 0–14 ms, respectively. The inhomogeneous broadening in this sample is $\simeq$1.0 cm^{-1}.

Part of the difficulty in using the 7009 Å/6934 Å data as a reliable measure of the mobility of single ions is the existence of excited states of the fourth-nearest-neighbor traps that are in near resonance with the R_1 frequency. Figure 11 shows that lowest lying excited states of the single-ion and N_1 and N_2 pair spectra. These states have been identified by Kisliuk *et al.*,[20] and must be optically connected with the ground states. As we have shown in Fig. 10, the direct excitation of the fourth-nearest-neighbor pair can be seen if we gate our electronics to look during the first few milliseconds following laser excitation where fast 1 msec N_2 decay is readily apparent. Since we normally gate our apparatus to look after 5 mesc, we can avoid seeing the direct excitation. However; *suppose that there are excited states that are not strongly optically connected with the ground state* but can be reached via a resonant transfer from an excited single Cr^{3+}. For example, using the notation of Kisliuk,[20] the fourth-nearest-neighbor excited state 4*I* has an energy (at 77 K) of 14418.2

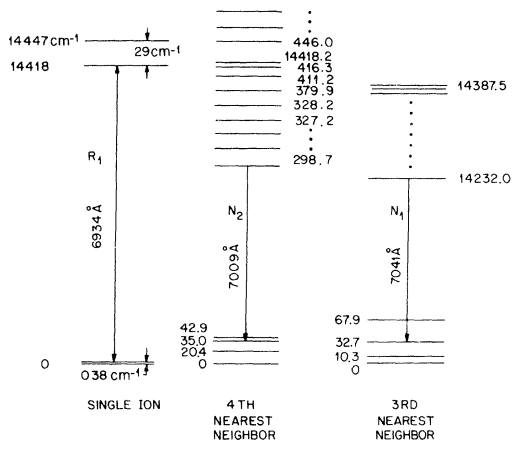

FIG. 11. Optically identified states of the lowest lying levels for single Cr^{3+} ions and the N_1 and N_2 pair states. The third-nearest-neighbor pair's spectrum (N_2) has no identified near-resonance states that are optically connected to the ground states.

cm^{-1}. The observed R_1 absorption frequency of 77 K for light polarization perpendicular and parallel to the z axis is 14418.16 and 14417.63 cm^{-1}, respectively. The excited states of the N_2 state have linewidths on the order of 1 cm^{-1}. (Recall that Fig. 10 shows an excited-state resonance of the N_2 trap that is roughly 1 cm^{-1} wide. Another excited state of N_2 located $\simeq 6.5$ cm^{-1} to the red of the inhomogeneous R_1 line also has an absorption width of $\simeq 1$ cm^{-1}.) Then by tuning the laser frequency in the vicinity of the R_1 inhomogeneous line, we may be tuning in and out of transfer resonances between single ions and the N_2 pair states.

The fact that we have failed to see the direct excitation of the $4I$ state may also be used to obtain a lower limit on the single-ion-to-trap transfer rate. The two paths for fourth-nearest-neighbor excitation are $N \rightarrow N^*$ (the $4I\,3$ transition) and $R \rightarrow R^* \rightarrow N^*$, where R^* and N^* indicates an excited state of R or N. The data of Fig. 10 and similar work by Selzer *et al.*[7] tells us that the probability for $R \rightarrow R^* \rightarrow N^*$ must be at least a factor of 10 larger than $N \rightarrow N^*$ since the 0.8 ms lifetime of the fourth-nearest-neighbor trap is not seen in time-resolved fluorescence studies. The total number of excitations $N \rightarrow N^*$ is proportional to $6[R]^2\sigma_{N\rightarrow N^*}\rho_{\mathrm{Al}}$, where $[R]$ is the fractional ruby concentration (0.0018, in our case), ρ_{Al} is the number density of Al ions in sapphire, $\sigma_{N\rightarrow N^*}$ is the optical cross section, and there are six equivalent fourth-nearest-neighbor pair sites.[20] Similarly,

$$R \rightarrow R^* \rightarrow N^* = (R \rightarrow R^*)(R^* \rightarrow N^*)$$
$$= (\rho_{\mathrm{Al}}[R]\sigma_{R\rightarrow R^*})(1 - e^{-4\pi/3\rho_N r_{\mathrm{eff}}^3}) .$$

In the last expression, we are saying that R^* will transfer to N^* if the probability for a trap found within a distance r_{eff} from an arbitrary single ion is at least 0.5. If r_{eff} turns out to be large, failure to see $N \rightarrow N^*$ must be taken as evidence for a large $R^* \rightarrow N^*$, and an excessively probable $R^* \rightarrow N^*$ may demand rapid R to R transfer. Quantitatively,

$$\frac{R \rightarrow R^* \rightarrow N^*}{N \rightarrow N^*} \simeq \frac{\sigma_{R\rightarrow R^*}\rho_{\mathrm{Al}}[R](1 - e^{-4\pi/3\rho_N r_{\mathrm{eff}}^3})}{\sigma_{N\rightarrow N^*}\rho_{\mathrm{Al}}6[R]^2}$$
$$\simeq \left(\frac{\sigma_{R\rightarrow R^*}}{\sigma_{N\rightarrow N^*}}\right)\frac{4\pi}{3}[R]\rho_{\mathrm{Al}}r_{\mathrm{eff}}^3 \simeq 10 .$$

We estimate that $\sigma_{R\rightarrow R^*}/\sigma_{N\rightarrow N^*} \simeq 10$ based on the lifetimes of the R and N states and the relative branching ratios for $\Delta S = 0$ and $\Delta S = 1$ transitions for fourth-nearest-neighbor pair states. Thus, one finds that $r_{\mathrm{eff}} \gtrsim 14$ Å, a range that is completely compatible with direct $R^* \rightarrow N^*$ feeding only. Note that if the lower limit on r_{eff} turned out to be a factor of 3 larger, a strong case could be made for fast $R \rightarrow R$ transfer.

We have also studied the N_1/R_1 fluorescence ratio (7014 Å/6934 Å) corresponding to single-ion transfer to third-nearest-neighbor pairs. There are no identified near-resonant states in the N_1 spectrum, and even if there are nonoptically connected states in the vicinity of the R_1 line, the likelihood of a duplication of the N_1 spectra is highly unlikely. Thus, the N_1/R_1 fluorescence ratio should be a better indicator of single-ion—single-ion transfer since the transfer of energy from single ion to N_1 trap is not complicated by near-resonance excited states of the trap. This study was hampered by background from the large phonon tail in the R_1 fluorescence (vibrational side bands) at 7041 Å and some care was needed in subtracting out this background. The background fluorescence was measured by scanning the spectrometer in the vicinity of 7041 Å. A resonance appears above a smooth, monotonically increasing background. Figure 12 indicates how the signal-to-background ratio is determined. Figure 13 shows the ratio data as a function of laser frequency; comparison can be

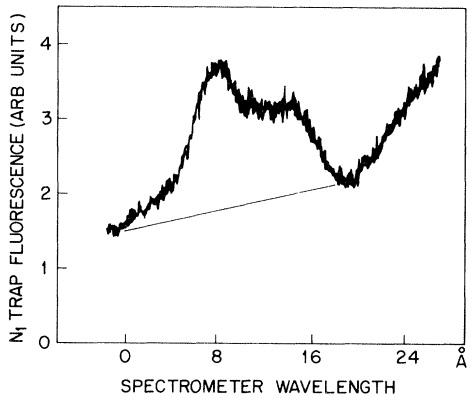

FIG. 12. Spectrometer scan in the frequency region around 7041 Å. The N_1 trap fluorescence is seen above the phonon tail of the R_1 fluorescence, and the straight line indicates how the R_1 fluorescence background is separated from the trap fluorescence. Laser excitation is near the center of the R_1 line at 6934 Å. Spectrometer resolution is $\simeq 1.5$ Å.

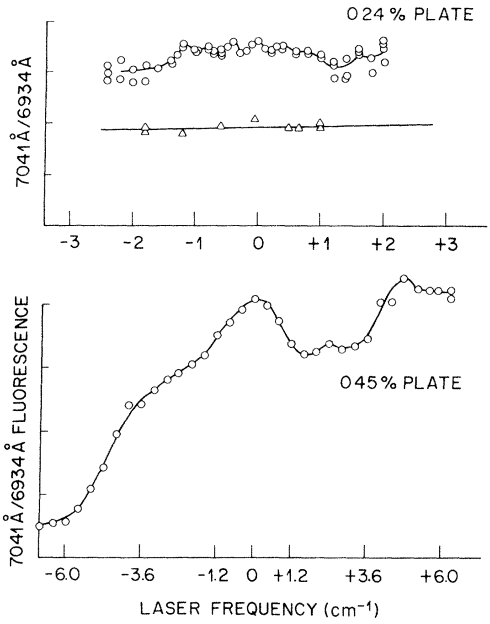

FIG. 13. N_1/R_1 fluorescence spectra as a function of laser frequency. The horizontal line in the 0.24 wt. % plate data marks the background level due to the phonon tail of the 6934 Å radiation. The background level in the 0.45 wt. % plate is less than 10% of the 7041 Å fluorescence.

made to the corresponding N_2/R_1 curves in Fig. 5. The N_1/R_1 ratio data show obvious differences from the N_2/R_1 data. The 0.24 wt. % sample gives only small modulations in the N_1/R_1 ratio when compared to the N_2/R_1 ratio. Similar behavior is also seen in lower concentration samples. Since the N_2/R_1 and N_1/R_1 curves are different at concentrations of 0.25 wt. % or lower, we must conclude that the N_1/R_1 and N_2/R_1 ratios cannot both be good measures of the single-ion—single-ion mobility, casting further doubt on KWG interpretation of the N_2/R_1 curves. However, we iterate again that the interpretation of the 7041 Å data depends on the background subtraction. If the broad plateau shown in Fig. 12 is part of the phonon sideband, the small variations in the N_1/R_1 ratio may be comparable with the variations in the N_2/R_1 ratio.

SUMMARY

Extensive measurements of the N_2/R_1 fluorescence ratio as a function of laser frequency in both powder and platelet samples do no duplicate the results of the KWG experiment. The major differences in our data can be summarized as follows: (1) Changes in the N_2/R_1 ratio appear in all concentrations from 0.035 wt. % powder to 0.45 wt. % platelets. (2) These changes are not sharp "breaks" and must be characterized as gradual changes. (3) The changes in the N_2/R_1 ratio do not move out with the concentration, and are consistent with a roughly universal curve. (4) Our changes in the N_2/R_1 ratio show greater modulations than the KWG data.

Thus, we find no clear evidence of a mobility edge, and although the N_2/R_1 ratios reflect the ability of a single ion to transfer to a trap, no conclusions can be made about the single-ion—single-ion transfer. Careful studies using samples at 0.18 wt. % concentration of different powder sizes show that a small amount of radiative trapping does not alter the basic shape of the N_2/R_1 curve. The nonradiatively trapped powder sample shows and N_2/R_1 ratio very similar to the 40 μm size sample, although the larger powder sample has a lifetime $\simeq$10% longer than the 3 μm size sample. Finally, there are unexplained features as large as any candidate for a mobility edge break. Therefore, any such interpretation is unwarranted. Studies of the N_1/R_1 ratio, although not conclusive, must cast further doubt on the KWG interpretation.

After the bulk of these measurements were made, more direct means were used to measure the single-ion—single-ion transfer. By extending the time-resolved fluorescence line-narrowing techniques used by Szabo[14,15] and Selzer and Yen,[7,21] we have been able to determine the fraction of ions that participate in fast nonradiative resonant transfer.[22] Also, by using an electric field switching technique, we have measured directly the times involved in transfer process.[23] These experiments force us to conclude that the probability of resonant nonradiative transfer is much smaller than previously thought. *In fact, in the lifetime of R_1 excitation, there is on the average only one energy transfer between single ions in samples of 0.25 wt. % concentration.*

There are still many unanswered questions concerning energy transfer in ruby. For example, can a frequency-*independent* $R \rightarrow N$ transfer and the measured frequency-*dependent* $R \rightarrow R$ transfer[22] account for the frequency dependence of the N_2/R_1 ratio, or does one have to use the idea of resonant transfer to a postulated excited state of the N_2 trap? Based on our E-field switching results, can one account for both the *shape* of the R_1 and N_2 decay curves and the absolute magnitude of the R_1

and N_2 fluorescence? Can we explain the shortened R_1 decay lifetime at concentrations $\gtrsim 0.5$ wt. % even though there is no dramatic increase in the amount of detected resonant nonradiative transfer? Finally, why should the N_1/R_1 and N_2/R_1 ratio curves be different at moderate or low concentration ruby ($\lesssim 0.25$ wt. %) but similar for 0.45 wt. % concentration samples? (Compare Figs. 13 and 5, especially within ± 3 cm^{-1} of line center.) We will address these questions in a subsequent publication.

We wish to acknowledge many informative discussions with S. Geschwind. We also thank S. L. McCall, P. Hu, R. Orbach, P. Liao, W. M. Yen, M. D. Sturge, G. F. Imbusch, R. J. Birgeneau, J. Koo, and L. R. Walker for numerous discussions, F. Robinson for polishing the ruby platelets, and S. Vincent for determining the Cr concentrations.

[1]J. Koo, L. R. Walker, S. Geschwind, Phys. Rev. Lett. 35, 1669 (1975).

[2]See, for example, N. F. Mott and E. A. Davis, *Electronic Processes in Non-Crystalline Materials,* 2nd ed., (Clarendon, Oxford, 1979).

[3]D. D. Smith, R. D. Mead, and A. H. Zewail, Chem. Phys. Lett. 50, 358 (1977).

[4]J. Klafter and J. Jortner, J. Chem. Phys. 68, 1513 (1978).

[5]C. Hsu and R. C. Powell, Phys. Rev. Lett. 35, 734 (1975).

[6]G. F. Imbusch, Phys. Rev. 135, 326 (1967).

[7]P. M. Selzer, D. S. Hamilton, and W. M. Yen, Phys. Rev. Lett. 38, 858 (1977); P. M. Selzer, D. L. Huber, B. B. Barnett, and W. M. Yen, Phys. Rev. B 17, 4979 (1978).

[8]R. J. Birgeneau, J. Chem. Phys. 50, 4282 (1969).

[9]A. Monteil and E. Duval, J. Lumin. 18/19, 793 (1979); J. Phys. C 12, L415, (1979).

[10]S. K. Lyo, Phys. Rev. B 3, 3331 (1971).

[11]P. W. Anderson, Phys. Rev. 109, 1492 (1958).

[12]P. W. Anderson, Comments Solid State Phys. 2, 193 (1970).

[13]J. Heber and H. Murmann, Z. Phys. B 26, 145 (1977).

[14]A. Szabo, Phys. Rev. Lett. 25, 924 (1970).

[15]A. Szabo, Phys. Rev. Lett. 27, 323 (1971); Phys. Rev. B 11, 4512 (1975).

[16]I. Ya Gerlovin, Fiz. Tverd. Tela (Leningrad) 16, 607 (1974) [Sov. Phys.—Solid State 16, 397 (1974)].

[17]P. F. Liao, L. M. Humphrey, D. M. Bloom, and S. Geschwind, Phys. Rev. B 20, 4145 (1979).

[18]D. S. Hamilton, D. Heiman, J. Feinberg, and R. W. Hellwarth, Opt. Lett. 4, 124 (1979).

[19]H. J. Eichler, J. Eichler, J. Knof, and Ch. Noack, Phys. Status Solidi A 52, 481 (1979).

[20]P. Kisliuk, N. C. Chang, P. L. Scott, and M. H. L. Pryce, Phys. Rev. 184, 367 (1969).

[21]P. M. Selzer and W. M. Yen, Opt. Lett. 1, 90 (1977).

[22]S. Chu, H. M. Gibbs, S. L. McCall, and A. Passner, in press.

[23]S. Chu, H. M. Gibbs, S. L. McCall, and A. Passner, Phys. Rev. Lett. 45, 1715 (1980).